International Journal of Fluid Mechanics Research, Vol. 33, No. 3, 2006

Mixed Convection Boundary Layer Flow of a Micropolar Fluid Along a Vertical Cylinder[†]

Rama Subba Reddy Gorla
Department of Mechanical Engineering
Cleveland State University
Cleveland, Ohio 44115

H. S. Takhar
Department of Engineering
Manchester Metropolitan University
Manchester M1 5GD, United Kingdom

A. J. Chamkha
Manufacturing Engineering Department
Public Authority for Applied Education and Training
P. O. Box 42325, Shuweikh 70654, Kuwait

The steady mixed convection boundary layer flow of a micropolar fluid along a vertical cylinder is studied for isothermal as well as uniform surface heat flux boundary conditions. The transformed conservation equations of the nonsimilar boundary layers are solved numerically using the Keller box scheme. Numerical solutions for the velocity, angular velocity, and temperature fields are presented for different values of the material and mixed convection parameters. The wall shear stress and the surface heat transfer rate increase with buoyancy and cylindrical curvature.

* * *

Nomenclature

C_f	local friction coefficient $\tau_{w*}(\rho U_\infty^2/2)^{-1}$;
f	dimensionless velocity function;
g	dimensionless microrotation;
g_0	acceleration due to gravity $[\mathrm{m/s^2}]$;
h	heat transfer coefficient $[\mathrm{W/(m^2K)}]$;
j	microinertia per unit mass $[\mathrm{m^2}]$;
k	thermal conductivity $[\mathrm{W/(mK)}]$;
N	angular velocity $[\mathrm{rad/s}]$;

[†]Received 09.11.2005

ISSN 1064-2277

Nu	Nusselt number hx/k_f;
Pr	Prandtl number $C_P\mu/k$;
R	radial coordinate $[\mathrm{m}]$;
R	radius of the cylinder $[\mathrm{m}]$;
Re	Reynolds number $U_\infty R/\nu$;
T	temperature [K];
u	velocity in x-direction $[\mathrm{m/s}]$;
v	velocity in r-direction $[\mathrm{m/s}]$;
U_∞	free stream velocity $[\mathrm{m/s}]$;
x	axial coordinate $[\mathrm{m}]$;
CWT	constant wall temperature;
CHF	constant heat flux;
Gr	Grashof number $g_0\beta R^3(T_w - T_\infty)/\nu^2$;
Gr^*	modified Grashof number $g\beta q_w R^4/(K_f\nu^2)$.

Greek Symbols

α	thermal diffusivity $[\mathrm{m}^2/\mathrm{s}]$;
β	volumetric coefficient of expansion $[1/\mathrm{K}]$;
γ	spin gradient viscosity $(\mu + \kappa/2)j$, $[\mathrm{kgm/s}]$;
Δ, λ	dimensionless material properties κ/μ, $\gamma/\mu j$;
θ	dimensionless temperature;
κ	vortex viscosity $[\mathrm{kg}/(\mathrm{ms})]$;
μ	dynamic viscosity $[\mathrm{kg}/(\mathrm{ms})]$;
ν	kinematic viscosity $[\mathrm{m}^2/\mathrm{s}]$;
ρ	density of fluid $[\mathrm{kg}/\mathrm{m}^3]$;
ψ	stream function $R(\nu U_\infty x)^{1/2} f(\xi, \eta)$;
ξ, η	dimensionless coordinates;
σ	buoyancy parameter (for CWT and CHF);
τ	shear stress $[\mathrm{Pa}]$.

Subscripts

f	fluid properties;
w	conditions at the surface of the cylinder;
∞	free stream conditions.

Introduction

Introduction It is well known that the classical Navier – Stokes theory does not adequately describe the flow properties of polymeric fluids, colloidal suspensions, and some naturally occurring fluids such as animal blood and fluids containing certain additives. Such fluids, which display certain microscopic effects arising from the local structure and microrotations of fluid elements, are known as micropolar fluids. They exhibit microrotational effects and microrotational inertia and can support couple stresses and body couples only. Eringen [1] proposed the theory of micropolar fluids, which shows microrotation effects as well as microinertia. The theory of thermomicropolar fluids was developed by Eringen [2] by extending the theory of micropolar fluids. The theory of micropolar fluids is generating a lot of interest, and many classical flows are being reexamined to

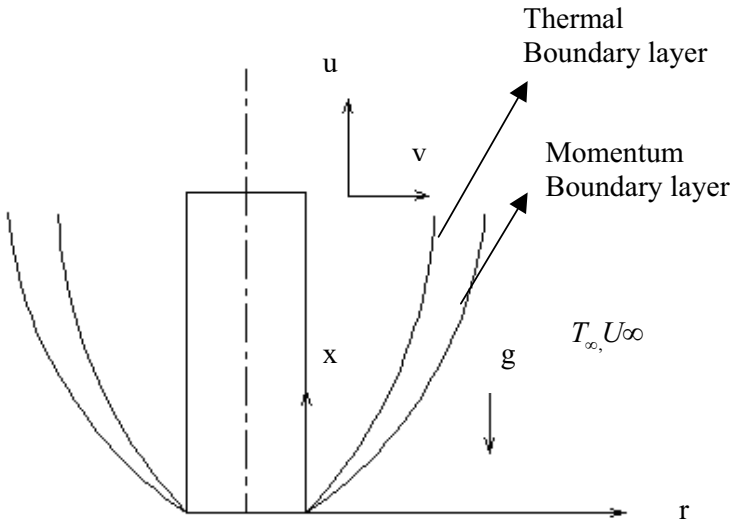

Fig. 1. The coordinate system and flow configuration.

determine the effects of fluid microstructure. A review made by Ariman et al. [3], the book written by Lukaszewicz [4], and the recent papers by Gorla [5–13], Gorla and Hassanien [14, 15], Gorla and Takhar [16], Gorla and Nashery [17], Gorla et al. [18–20], and other researchers [21–32] clearly show the fast development of the theory of micropolar fluids.

Mixed convection flows constitute an important area of heat transfer problems. Gebhart et al. [33] presented an excellent literature survey for Newtonian fluids. Mansour and Gorla [34] analyzed the problem of magnetohydrodynamic (MHD) mixed convection near the lower stagnation point of a circular cylinder immersed in a micropolar fluid. The literature on mixed convection in micropolar fluids is scarce.

The present work was undertaken in order to examine the steady mixed convection boundary layer flow of a micropolar fluid along a vertical cylinder. The governing nonsimilar boundary layer equations are solved numerically. At a distance far away from the leading edge the boundary layer develops a two-layer structure. This structure is analyzed by means of asymptotic methods. Numerical results for the velocity, microrotation, and temperature fields are presented for a wide range of the material properties of the fluid.

1. Statement of the Problem

Let us consider a vertical cylinder of radius R, which is aligned parallel to a uniform free stream of an incompressible, micropolar fluid flow with velocity U_∞ and temperature T_∞. Let x and r denote the streamwise and radial coordinates, respectively, and let the gravitational force act in the direction opposite to the x coordinate. Fig. 1 shows the flow model and coordinate system. The buoyancy force then acts in the same direction as the forced flow when $T_W > T_\infty$ and in the opposite direction to the forced flow when $T_W < T_\infty$. The former is referred to as assisting flow and the latter as opposite flow.

The field equation of an incompressible, axisymmetric, steady, laminar, incompressible, micropolar fluid flow may be expressed within boundary layer approximation as follows:

mass

$$\frac{\partial(ru)}{\partial x} + \frac{\partial(rv)}{\partial r} = 0, \tag{1}$$

momentum

$$u\frac{\partial u}{\partial x} + v\frac{\partial u}{\partial r} = \left(\nu + \frac{\kappa}{\rho}\right)\frac{1}{r}\frac{\partial}{\partial r}\left(r\frac{\partial u}{\partial r}\right) + \frac{\kappa}{\rho}\left(\frac{N}{r} + \frac{\partial N}{\partial r}\right) + g_0\beta(T - T_\infty), \tag{2}$$

angular momentum

$$u\frac{\partial N}{\partial x} + v\frac{\partial u}{\partial r} = \frac{\gamma}{\rho j}\left[\frac{1}{r}\frac{\partial}{\partial r}\left(r\frac{\partial N}{\partial r}\right) - \frac{N}{r^2}\right] - \frac{\kappa}{\rho}\left(\frac{\partial u}{\partial r} + 2N\right), \tag{3}$$

energy

$$u\frac{\partial T}{\partial x} + v\frac{\partial T}{\partial r} = \frac{\alpha}{r}\frac{\partial}{\partial r}\left(r\frac{\partial T}{\partial r}\right). \tag{4}$$

In the above equations, u and v are the velocity components in the x and r directions, N is the component of microrotation, T is the fluid temperature, g_0 is the gravitational acceleration, and β is the volumetric coefficient of thermal expansion. The boundary condition for the velocity field may be written as

$$\begin{aligned} &r = R: \qquad u = v = 0, \qquad N = -n\left(\frac{\partial u}{\partial r}\right), \\ &r \to \infty \qquad u \to U_\infty, \qquad N \to 0. \end{aligned} \tag{5}$$

For the temperature field, we have

$$\begin{aligned} &\text{at} \quad r = R, \qquad T = T_w \text{ (isotherm. wall)} \quad \text{or} \quad q_w = -k_f\frac{\partial T}{\partial r} \text{ (const. surf. heat flux)}, \\ &\text{as} \quad r \to \infty, \qquad\qquad\qquad\qquad T \to T_\infty. \end{aligned} \tag{6}$$

We follow Gorla et al. [19] by assigning a variable relation between microrotation and the surface skin friction, where n is a constant and varies from 0 to 1. The value $n = 0$ represents concentrated particle flows, in which the particle density is sufficiently great that microelements close to the wall are unable to rotate. This condition is also called the strong interaction. The case corresponding to $n = 0.5$ results in the vanishing of antisymmetric parts of the stress tensor and represents weak concentration. In this case, the particle rotation is equal to fluid vorticity at the boundary for fine-particle suspension. When $n = 1$, we have flows that are representative of turbulent boundary layers. The case of $n = 0.5$ is considered in the present paper.

It is implied that the microinertia j is constant and that the microstructure spin effect is included. We assume that the coefficients of viscosity are related as (see [35])

$$\gamma = \left(\mu + \frac{\kappa}{2}\right)j. \tag{7}$$

Now, we define a stream function $\psi(x, r)$ such that $ru = \partial\psi/\partial r$ and $rv = -\partial\psi/\partial x$. It may be

verified that the continuity equation is automatically satisfied. We further define

$$\xi = \frac{4}{R}\left(\frac{\nu x}{U_\infty}\right)^{1/2}, \qquad \eta = \left(\frac{U_\infty}{\nu x}\right)^{1/2}\left(\frac{r^2 - R^2}{4R}\right),$$

$$\psi = R(\nu U_\infty x)^{1/2} f(\xi,\eta), \qquad N = \frac{R}{r}\left(\frac{U_\infty \nu}{R}\right)^{1/2}\frac{\rho}{4\kappa} g(\xi,\eta),$$

$$\theta = \begin{cases} \dfrac{T - T_\infty}{T_w - T_\infty} & \text{(isothermal case)}, \\ \dfrac{T - T_\infty}{q_w/k_f(\nu x/U_\infty)} & \text{(uniform heat flux case)}, \end{cases} \tag{8}$$

or

$$B = \frac{R^2}{j}, \qquad \Delta = \frac{\kappa}{\mu}, \qquad \lambda = \frac{\gamma}{\mu j} = 1 + \frac{\Delta}{2},$$

$$\mathrm{Gr} = \begin{cases} 16\mathrm{Re}\,\sigma & \text{(isothermal case)}, \\ \dfrac{g_0 \beta R^3 (T_w - T_\infty)}{\nu^2}. \end{cases}$$

1.1. Isothermal Wall Boundary Condition. Substituting the expressions (8) into Eqs (2) – (4), we obtain

$$(1+\Delta)\frac{\partial}{\partial\eta}[(1+\xi\eta)f''] + ff'' + g' + 8\xi^2\sigma\theta = \xi\left[f'\frac{\partial f'}{\partial\xi} - f''\frac{\partial f}{\partial\xi}\right], \tag{9}$$

$$\begin{aligned}\left(1+\frac{\Delta}{2}\right)(1+\xi\eta)g'' + gf' + fg' = \frac{\Delta^2 B}{4}\xi(1+\xi\eta) + \frac{\Delta B}{2}\xi^2 g \\ + \frac{\xi^2 g}{2}\frac{\partial f}{\partial\xi} - \frac{\xi g}{2}(\eta f' - f) + \xi\left[f'\frac{\partial g}{\partial\xi} - g'\frac{\partial f}{\partial\xi}\right],\end{aligned} \tag{10}$$

$$\frac{1}{\mathrm{Pr}}(1+\xi\eta)\theta'' + \left(f + \frac{\xi}{\mathrm{Pr}}\right)\theta' = \xi\left[f'\frac{\partial\theta}{\partial\xi} - \theta'\frac{\partial f}{\partial\xi}\right]. \tag{11}$$

In the above equations, a prime denotes differentiation with respect to η only. The transformed boundary conditions for the velocity and temperature fields are given by

$$\begin{aligned} f(\xi,0) = f'(\xi,0) = 0, \qquad & f'(\xi,\infty) = 1; \\ g(\xi,0) = -n\Delta f''(\xi,0), \qquad & g(\xi,\infty) = 0; \\ \theta(\xi,0) = 1, \qquad & \theta(\xi,\infty) = 0. \end{aligned} \tag{12}$$

1.2. Constant Surface Heat Flux Boundary Condition. For this case, we define the dimensionless temperature

$$\theta = \frac{T - T_\infty}{2q_w/k_f(\nu x/U_\infty)}, \qquad \sigma = \frac{\mathrm{Gr}^*}{8\mathrm{Re}}, \qquad \mathrm{Gr}^* = \frac{g\beta q_w R^4}{K_f \nu^2}.$$

Substituting expressions (8) into Eqs (2) – (4), the momentum and energy equations may be written as

$$(1+\Delta)\frac{\partial}{\partial\eta}[(1+\xi\eta)f'']+ff''+g'+2\xi^3\sigma\theta=\xi\left[f'\frac{\partial f'}{\partial\xi}-f''\frac{\partial f}{\partial\xi}\right], \tag{13}$$

$$\frac{1}{\mathrm{Pr}}(1+\xi\eta)\theta''+\left(f+\frac{\xi}{\mathrm{Pr}}\right)\theta'-f'\theta=\xi\left[f'\frac{\partial\theta}{\partial\xi}-\theta'\frac{\partial f}{\partial\xi}\right]. \tag{14}$$

The transformed angular momentum equation is the same as Eq. (10) and is therefore not reproduced here. The transformed boundary conditions for the velocity and angular velocity fields are the same as Eq. (12). The transformed boundary conditions for the temperature field are given by

$$\theta'(\xi,0)=-1, \qquad \theta(\xi,\infty)=0. \tag{15}$$

2. Asymptotic Solution for Main Layer

The governing equations of the problem are solved numerically by the Keller box method, which is an implicit scheme with unconditional stability. The method allows for nonuniform grid discretization and converts the differential equations into algebraic ones, which are then solved by the Thomas algorithm. We have used 30 grid points in the ξ direction and 196 points in the η direction. Variable step sizes in the η direction with an initial step of 0.001 and a growth factor of 1.03 and constant step sizes of 0.01 in the ξ direction are employed. A mesh sensitivity exercise has been performed to ensure grid independence. The solution convergence criterion required that the difference between current and previous iterations be 10^{-5}.

Now, define $h=g+f''/2$. We set the main layer Eqs (9) – (12) in the following expansion:

$$f(\xi,\eta)=F_0(\eta)+\xi^{-1/2}F_1(\eta)+\ldots, \tag{16}$$

$$h(\xi,\eta)=\xi^{-1}H_0(\eta)+\xi^{-3/2}H_1(\eta)+\ldots, \tag{17}$$

$$\theta(\xi,\eta)=\theta_0(\eta)+\xi^{-1/2}\theta_1(\eta)+\ldots \tag{18}$$

When expressions (16) – (18) are substituted into Eqs (9) – (11) and terms involving equal powers of ξ are equated to zero, one obtains a set of ordinary differential equations governing the momentum, angular momentum, and thermal fields, and these equations have been solved on the computer using Mathematica. These details may be summarized as

$$\left[(1+\Delta)-\frac{1}{2}\right]F_0'''+F_0F_0''+8\sigma\theta_0=0, \tag{19}$$

$$\left[(1+\Delta)-\frac{1}{2}\right]F_1'''+F_0F_1''+F_1F_0''+8\sigma\theta_1+\frac{1}{2}F_0'F_1'=0, \tag{20}$$

$$\left(1+\frac{\Delta}{2}\right)H_0''+2H_0F_0'-F_1''F_1'+F_0H_0'=0, \tag{21}$$

Table 1
Values of $\theta_0'[x]$, $F_0''[0]$, $\theta_1'[0]$, and $F_1''[0]$ are obtained considering $\mathrm{Pr} = 0.72$ and $\sigma = 0.1$, and applying various values of Δ.

Δ	$\theta_0'[x]$	$F_0''[0]$	$\theta_1'[0]$	$F_1''[0]$
0	-0.0202	0.5343	0.0141	0.0569
0.5	-0.0187	0.4121	0.0131	0.0372
1	-0.0172	0.3121	0.0114	0.0279
3	-0.0168	0.2183	0.0092	0.0145
5	-0.0155	0.1853	0.0095	0.0112
8	-0.0135	0.1642	0.0077	0.0066

Table 2
Values of $\theta_0'[x]$, $F_0''[0]$, $\theta_1'[0]$, and $F_1''[0]$ are obtained considering $\mathrm{Pr} = 10$ and $\sigma = 0.1$, and applying various values of Δ.

Δ	$\theta_0'[x]$	$F_0''[0]$	$\theta_1'[0]$	$F_1''[0]$
0	-0.0981	0.3523	0.4212	0.9811
0.5	-0.0972	0.2446	0.5928	0.9711
1	-0.0752	0.2285	0.8526	0.9379
3	-0.0712	0.1682	1.4121	0.9279
5	-0.0681	0.1453	1.8786	0.8814
8	-0.0652	0.1353	1.7834	0.5488

$$\frac{\theta_0''}{\mathrm{Pr}} + F_0\theta_0' = 0, \tag{22}$$

$$\frac{\theta_1''}{\mathrm{Pr}} + F_0\theta_1' + \frac{F_1\theta_0'}{2} + \frac{F_0'\theta_1}{2} = 0. \tag{23}$$

Now, for the main layer, the boundary conditions are

$$\begin{aligned} f(\xi,0) = f'(\xi,0) = 0, \qquad & f'(\xi,\infty) = 1; \\ h(\xi,0) = (1-\Delta/2)f''(\xi,0), \qquad & h(\xi,\infty) = 0; \\ \theta(\xi,0) = 1, \qquad & \theta(\xi,\infty) = 0. \end{aligned} \tag{24}$$

Eqs (19) – (23) were solved numerically. The missing wall values are tabulated for a range of material and buoyancy parameters (see Tables 1 – 4).

We now set the inner layer Eqs (9) – (11) in the following expansion:

$$\chi = \eta\xi + 1, \tag{25}$$

$$f(\xi,\chi) = \xi^{-2}F_0(\chi) + \xi^{-(5/2)}F_1(\chi) + \cdots, \tag{26}$$

Table 3
Values of $\theta_0'[x]$, $F_0''[0]$, $\theta_1'[0]$, and $F_1''[0]$ are obtained considering $\mathrm{Pr} = 0.72$ and $\sigma = 1$, and applying various values of Δ.

Δ	$\theta_0'[x]$	$F_0''[0]$	$\theta_1'[0]$	$F_1''[0]$
0	-0.00467	0.55420	0.0345	1.52310
0.5	-0.00380	0.31544	0.0382	1.48010
1	-0.00310	0.28310	0.0412	1.10110
3	-0.00250	0.19720	0.0506	0.87230
5	-0.00170	0.16540	0.0698	0.89812
8	-0.00150	0.15530	0.0752	0.65240

Table 4
Values of $\theta_0'[x]$, $F_0''[0]$, $\theta_1'[0]$, and $F_1''[0]$ are obtained considering $\mathrm{Pr} = 10$ and $\sigma = 1$, and applying various values of Δ.

Δ	$\theta_0'[x]$	$F_0''[0]$	$\theta_1'[0]$	$F_1''[0]$
0	-0.00981	0.48590	0.00948	0.1663
0.5	-0.00972	0.21544	0.00880	0.1781
1	-0.00830	0.19904	0.01710	0.2211
3	-0.00821	0.16720	0.02210	0.1523
5	-0.00754	0.11540	0.04980	0.2712
8	-0.00672	0.13530	0.06440	0.1988

$$\theta(\xi,\eta) = \xi^{-1/2}\theta_0(\chi) + \xi^{-1}\theta_1(\chi) + \cdots, \tag{27}$$

$$h(\xi,\eta) = H_0(\chi) + \xi^{-1/2}H_1(\chi) + \cdots \tag{28}$$

When expressions (25) – (28) are substituted into Eqs (9) – (11) and terms involving equal powers of χ are equated to zero, we get the following inner-layer equations:

$$[(1+\Delta)\chi - 1]F_0''' + H_0' = 0, \tag{29}$$

$$[(1+\Delta)\chi - 1]F_1''' + H_1' = 0, \tag{30}$$

$$\left[\left(1+\frac{\Delta}{2}\right)\chi\right]H_0'' = \frac{\Delta B}{2}H_0, \tag{31}$$

$$\left[\left(1+\frac{\Delta}{2}\right)\chi\right]H_1'' = \frac{\Delta B}{2}H_1, \tag{32}$$

$$(1+\chi)\theta_0'' + \theta_0' = 0, \tag{33}$$

$$(1+\chi)\theta_1'' + \theta_1' = 0. \tag{34}$$

The boundary conditions at $\chi = 1$ are

$$\begin{gathered} F_0 = F_0' = F_1 = F_1'' = 0, \qquad \theta_0 = 1, \qquad \theta_1 = 0, \\ H_0 = (1-\Delta/2)F_0'', \qquad H_1 = (1-\Delta/2)F_1''. \end{gathered} \tag{35}$$

The solutions are given by

$$H_0(\chi) = \frac{\sqrt{\chi}(1-\Delta/2)F_0''(0)}{-\gamma - \log_e(k/2) + 1/k}\left\{-\gamma - \log_e\frac{k\sqrt{\chi}}{2} + \frac{1}{k\sqrt{\chi}}\right\}, \tag{36}$$

$$\begin{aligned} F_0(\chi) = (1+\Delta)x + \frac{m\chi}{k} + \frac{2}{9}m\chi^{3/2} - \frac{2}{3}m\chi^{3/2}\gamma - \frac{2}{3}m\chi^{3/2}\log_e\frac{k\sqrt{\chi}}{2} + m\chi^{3/2}\log_e\chi \\ -F_0''(0)\left(1+\frac{3}{2}\Delta\right)\chi - \frac{m}{k} - \frac{2}{9}m + \frac{2m\gamma}{3} + \frac{2}{3}m\log_e\frac{k}{2} + F_0''(0)\left(1+\frac{3}{2}\Delta\right), \end{aligned} \tag{37}$$

$$\theta_0(\chi) = 1, \tag{38}$$

$$\theta_1(\chi) = 0, \tag{39}$$

$$\begin{aligned} F_1(\chi) = (1+\Delta)x + \frac{m\chi}{k} + \frac{2}{9}m\chi^{3/2} - \frac{2}{3}m\chi^{3/2}\gamma - \frac{2}{3}m\chi^{3/2}\log_e\frac{k\sqrt{\chi}}{2} + m\chi^{3/2}\log_e\chi \\ -F_1''(0)\left(1+\frac{3}{2}\Delta\right)\chi - \frac{m}{k} - \frac{2}{9}m + \frac{2m\gamma}{3} + \frac{2}{3}m\log_e\frac{k}{2} + F_1''(0)\left(1+\frac{3}{2}\Delta\right), \end{aligned} \tag{40}$$

where

$$k = \sqrt{\frac{B\Delta}{2+\Delta}}, \qquad m = \frac{(1-\Delta/2)F''(0)}{-\gamma - \log_e(k/2) - 1/k}.$$

3. Results and Discussion

The wall shear stress and wall couple stress are given by

$$\tau_w = [\mu + (1-n)\kappa]\frac{U_\infty}{4}\left(\frac{U_\infty}{\nu x}\right)^{1/2} f''(\xi, 0), \tag{41}$$

$$m_w = -\frac{\beta}{R}\left(\frac{U_\infty\nu}{x}\right)^{1/2}\frac{\rho}{4\kappa}g(\xi,0) - \frac{\gamma}{R}\left(\frac{U_\infty\nu}{x}\right)^{1/2}\frac{\rho}{4\kappa}g(\xi,0) + \gamma\left(\frac{U_\infty\nu}{x}\right)^{1/2}\frac{\rho}{8\kappa}g'(\xi,0), \tag{42}$$

$$C_f = \frac{\tau_w}{\rho U_\infty^2/2} = \frac{1}{2}[1+(1-n)\Delta]\mathrm{Re}_x^{-1/2} f''(\xi, 0), \tag{43}$$

where Re_x is the local Reynolds number and is given by

$$\mathrm{Re}_x = \frac{U_\infty x}{\nu}. \tag{44}$$

For the constant wall temperature case (CWT), we may write, by Fourier's law,

$$q_w(x) = -k_f \left(\frac{\partial T}{\partial r}\right)_{r=R} = -\frac{k_f(T_w - T_\infty)}{2} \left(\frac{U_\infty}{\nu x}\right)^{1/2} \theta'(\xi, 0). \tag{45}$$

The local heat transfer coefficient is given by

$$h(x) = \frac{q_w(x)}{T_w - T_\infty}\,. \tag{46}$$

The local Nusselt number for constant wall temperature (CWT) may be written as

$$\mathrm{Nu}_x = \frac{hx}{k_f} = -\frac{1}{2}\mathrm{Re}_x^{1/2}\theta'(\xi, 0). \tag{47}$$

For the constant wall heat flux (CWH) boundary condition, we may write for the local Nusselt number

$$\mathrm{Nu}_x = \frac{1}{2}\mathrm{Re}_x^{1/2}\frac{1}{\theta(\xi, 0)}\,. \tag{48}$$

Fig. 2 shows the velocity distribution within the boundary layer. As the material property parameter Δ increases, the velocity maxima decreases, and the velocity profiles become flatter. Fig. 3 shows the temperature profiles. As Δ increases, temperature increases, and the thermal boundary layer thickness increases. Fig. 4 shows the angular velocity profiles. As Δ increases, the absolute value of the microrotation component within the boundary layer increases.

Fig. 5 shows the results for the surface friction factor. As Δ increases, the friction factor increases along the streamwise distance. Fig. 6 displays results for the dimensionless heat transfer rate. As Δ increases, the heat transfer rate decreases with streamwise distance. Fig. 7 shows that the wall couple stress decreases with Δ along the streamwise length.

Figs 8 – 10 show the boundary layer profiles for various Prandtl numbers. As Pr increases, the velocity profiles become flatter, the temperature decreases, thermal boundary layer thickness diminishes, and the absolute value of the microrotation component increases. As the Prandtl number increases, the thermal diffusivity decreases when compared to momentum diffusivity. Figs 11 – 13 show results for the friction factor, Nusselt number, and wall couple stress. As Pr increases, the surface friction factor decreases, the surface heat transfer rate increases, and the wall couple stress decreases with streamwise distance. Figs 14 and 15 show results for the friction factor and the Nusselt number, with σ as the parameter. As σ, the buoyancy parameter, increases, the surface friction factor increases, and the surface heat transfer rate also increases.

Concluding Remarks

In this paper, we have studied the problem of steady, laminar, combined, convective flow of an incompressible micropolar fluid along a vertical cylinder. Numerical solutions are presented for the fluid flow and heat transfer characteristics, and their dependence on material parameters of the fluid has been discussed. As the Prandtl number increases, the surface friction factor decreases, the surface heat transfer rate increases, and the wall couple stress decreases with streamwise distance. It is found that a two-layer structure develops as the distance downstream increases. An asymptotic analysis of this structure is presented.

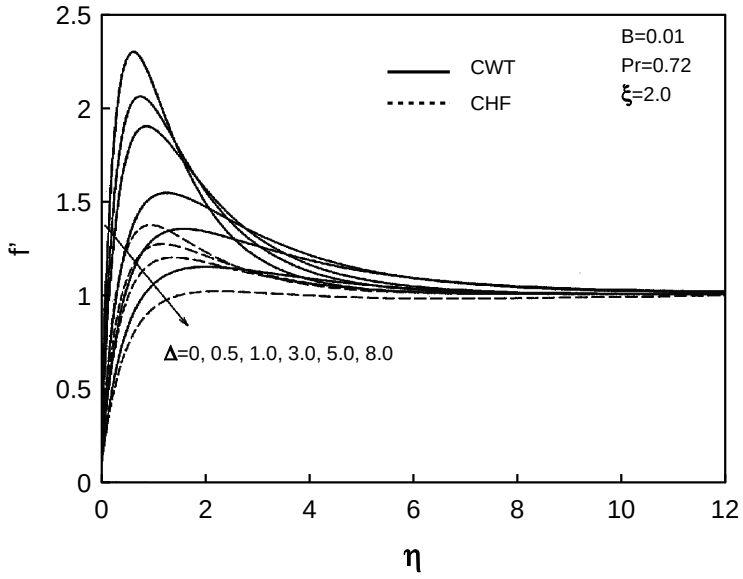

Fig. 2. Streamwise velocity distribution.

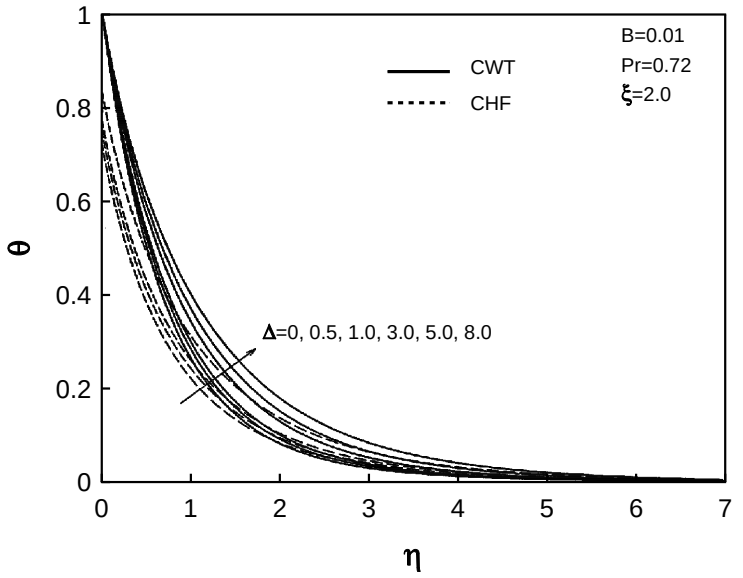

Fig. 3. Temperature distribution.

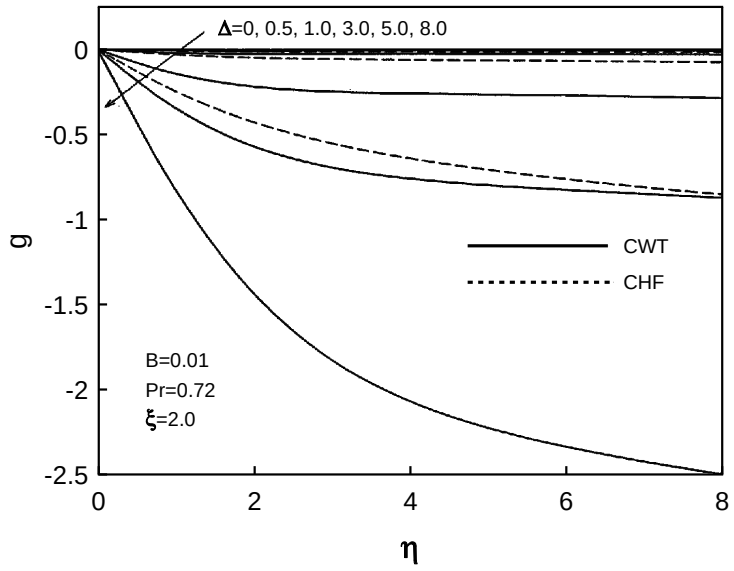

Fig. 4. Angular velocity distribution.

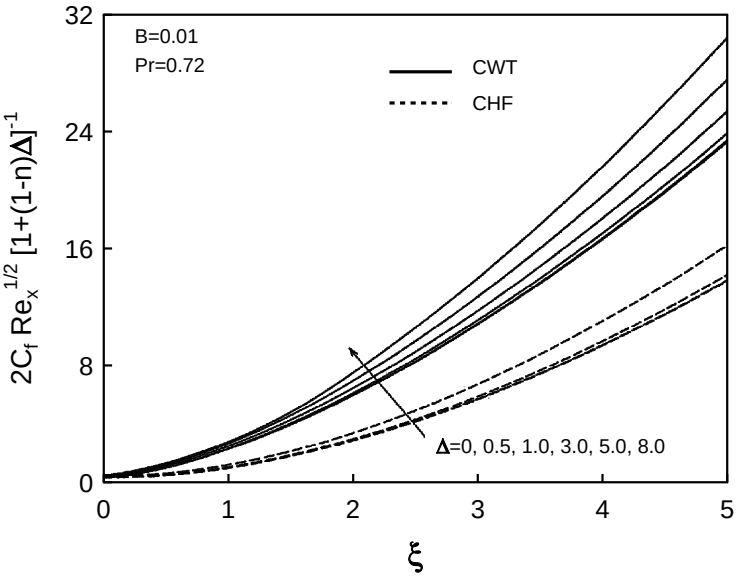

Fig. 5. Friction factor.

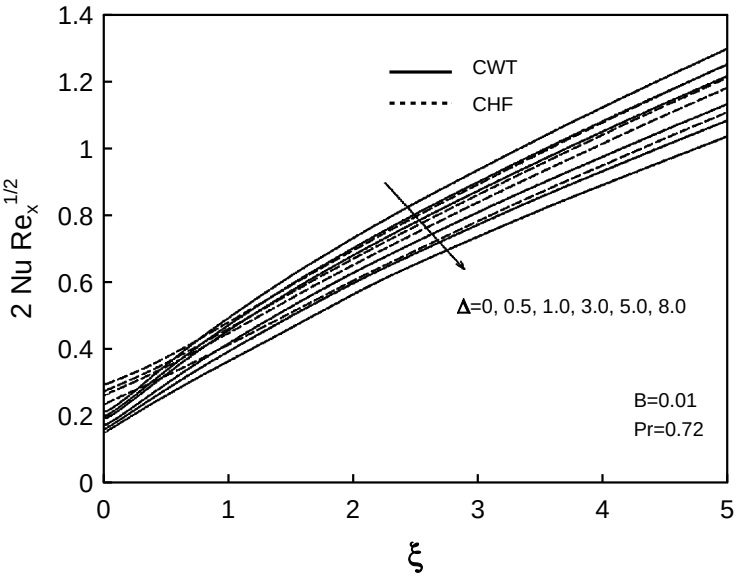

Fig. 6. Dimensionless heat transfer rate.

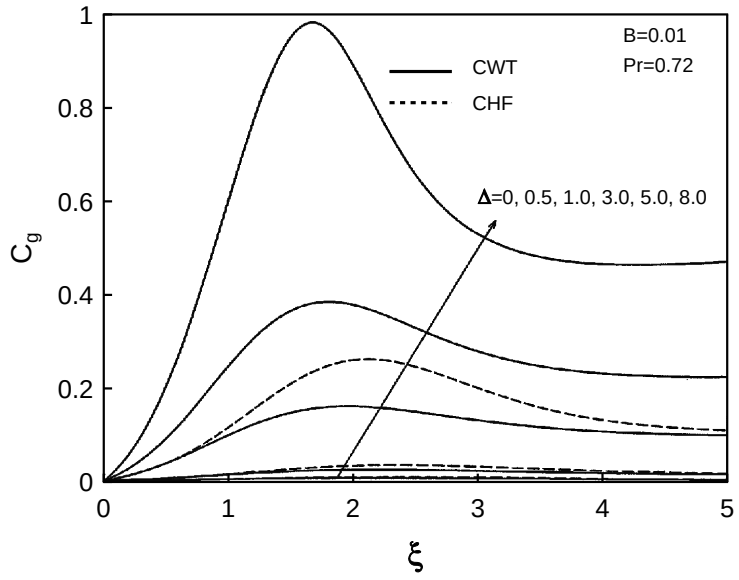

Fig. 7. Dimensionless wall couple stress.

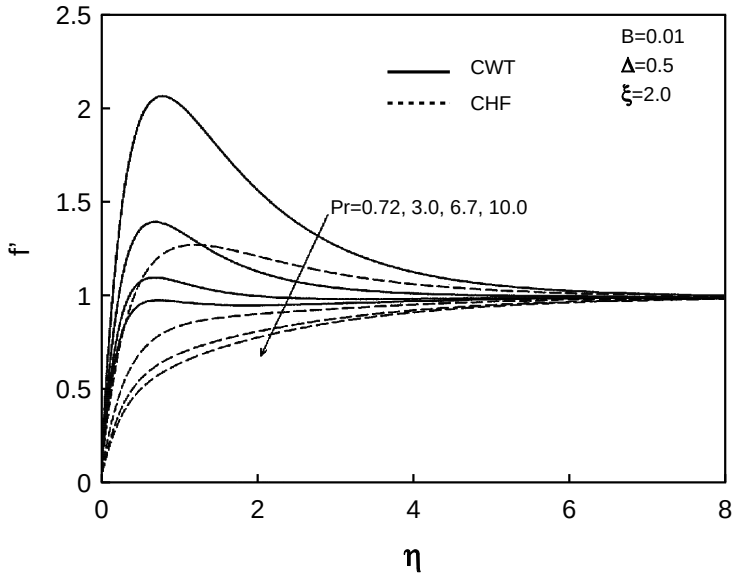

Fig. 8. Streamwise velocity distribution.

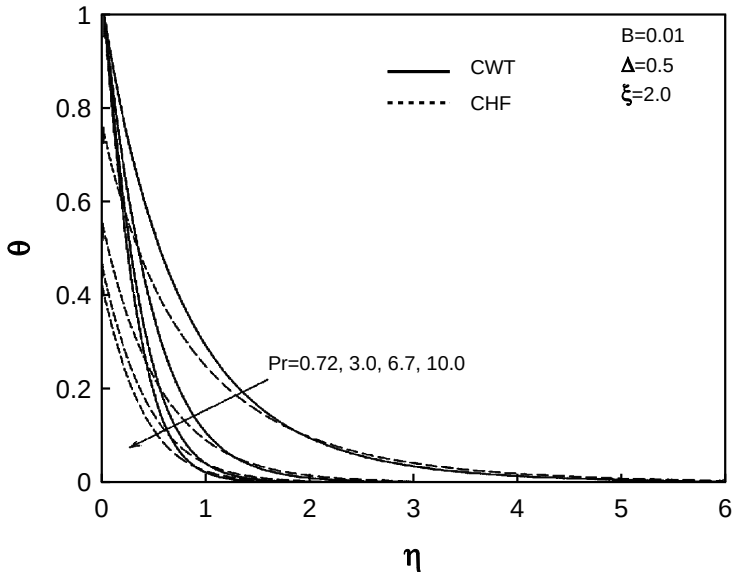

Fig. 9. Temperature distribution.

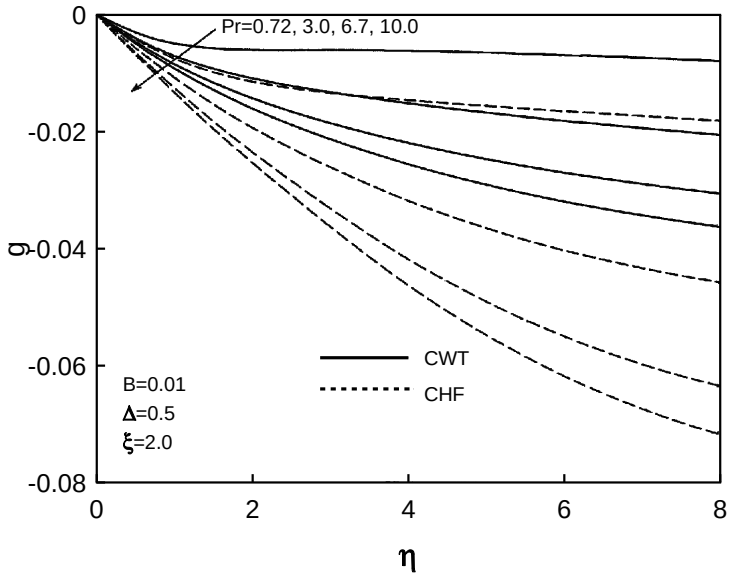

Fig. 10. Angular velocity distribution.

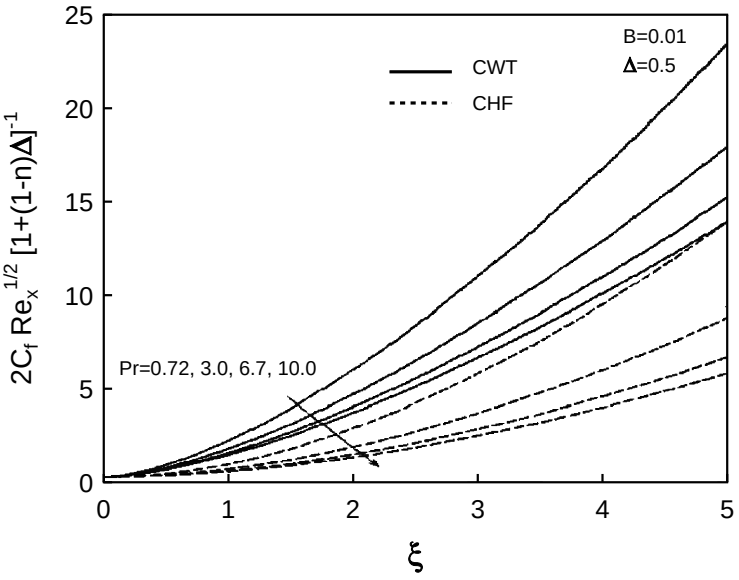

Fig. 11. Friction factor.

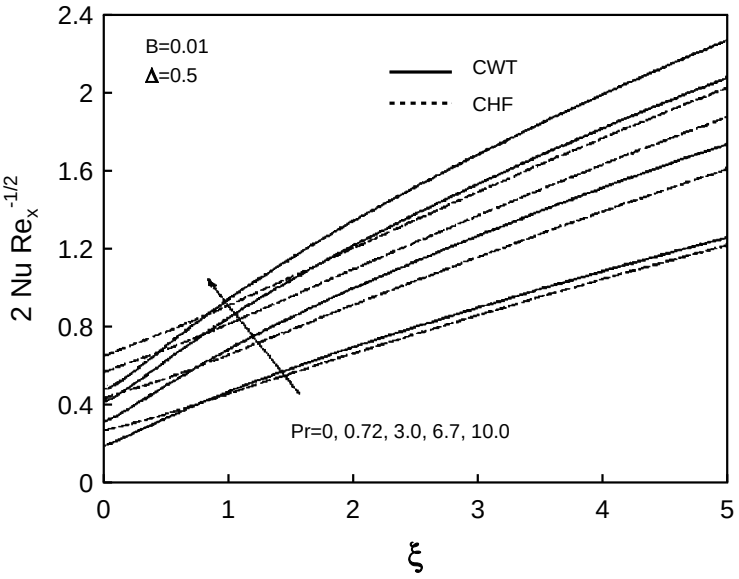

Fig. 12. Dimensionless heat transfer rate.

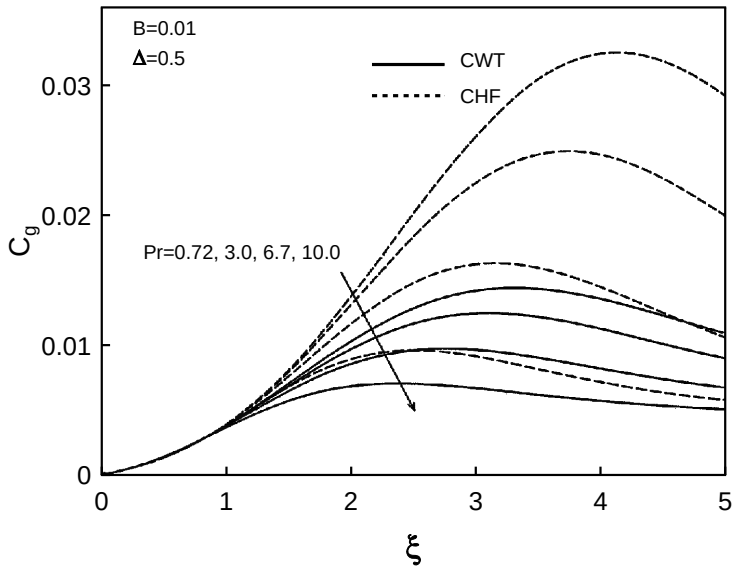

Fig. 13. Dimensionless wall couple rate.

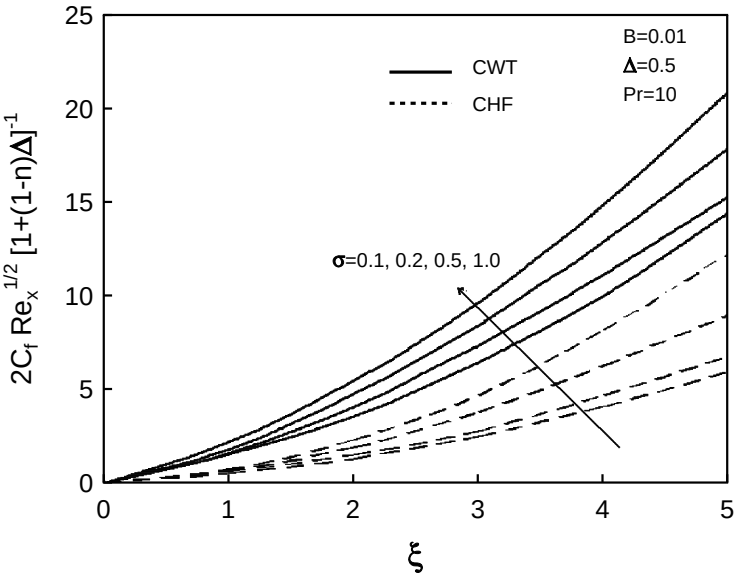

Fig. 14. Friction factor.

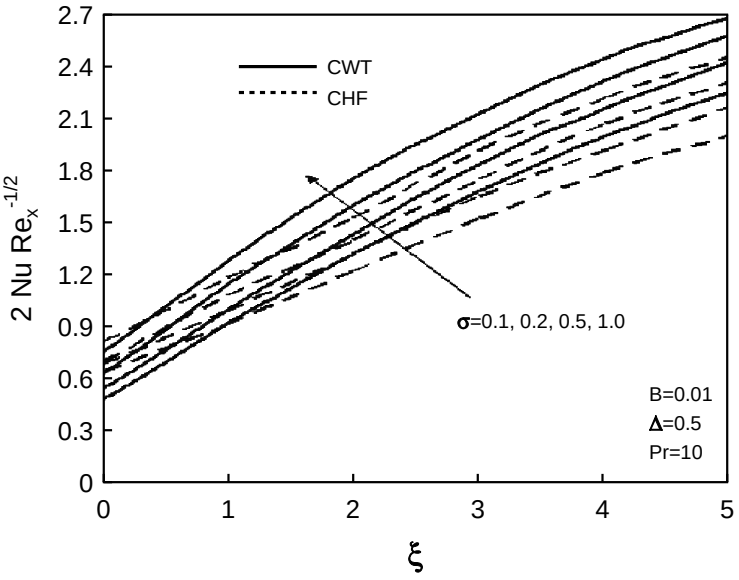

Fig. 15. Dimensionless heat transfer rate.

REFERENCES

1. Eringen, A. C., Theory of Micropolar Fluids, *J. Math. Mech.*, 1966, **16**, pp. 1–18.
2. Eringen, A. C., Theory of Thermomicropolar Fluids, *J. Math. Anal. Appl.*, 1972, **38**, pp. 480–496.
3. Ariman, T., Turk, M. A., and Sylvester, N. D., Microcontinuum Fluid Mechanics – A Review, *Int. J. Engng Sci.*, 1973, **11**, pp. 905–930.
4. Lukaszewicz, G., *Micropolar Fluids: Theory and Application*, Birkhauser, Basel, 1999.
5. Gorla, R. S. R., Thermal Boundary Layer of a Micropolar Fluid at a Stagnation Point, *Int. J. Engng Sci.*, 1980, **18**, pp. 611–617.
6. Gorla, R. S. R., Axisymmetric Thermal Boundary Layer of a Micropolar Fluid on a Cylinder, *Int. J. Engng Sci.*, 1985, **23**, pp. 401–407.
7. Gorla, R. S. R., The Axisymmetric Micropolar Boundary Layer on a Long Thin Cylinder, *Int. J. Engng Sci.*, 1984, **22**, pp. 293–300.
8. Gorla, R. S. R., Micropolar Boundary Layer at a Stagnation Point on a Moving Wall, *Int. J. Engng Sci.*, 1983, **21**, pp. 25–34.
9. Gorla, R. S. R., Boundary Layer Flow of a Micropolar Fluid in the Vicinity of an Axisymmetric Stagnation Point on a Cylinder, *Int. J. Engng Sci.*, 1990, **28**, pp. 145–152.
10. Gorla, R. S. R., Combined Forced and Free Convection in the Boundary Layer Flow of a Micropolar Fluid on a Continuous Moving Vertical Cylinder, *Int. J. Engng Sci.*, 1989, **27**, pp. 77–86.
11. Gorla, R. S. R., Buoyancy Effects on the Boundary Layer Flow of a Micropolar Fluid Along a Vertical Cylinder, *Int. J. Engng Sci.*, 1988, **26**, pp. 883–892.
12. Gorla, R. S. R., Unsteady Mixed Convection in Micropolar Boundary Layer Flow in a Vertical Plate, *Int. J. Fluid Dyn. Resch*, 1995, **15**, pp. 237–250.
13. Gorla, R. S. R., Mixed Convection in a Micropolar Fluid from a Vertical Surface with Uniform Heat Flux, *Int. J. Engng Sci.*, 1992, **30**, pp. 349–358.
14. Gorla, R. S. R. and Hassanien, I. A., Mixed Convection Boundary Layer Flow of a Micropolar Fluid Near a Stagnation Point on a Horizontal Cylinder, *Int. J. Engng Sci.*, 1990, **28**, pp. 153–162.
15. Gorla, R. S. R. and Hassanien, I. A., Combined Forced and Free Convection in Stagnation Flows of Micropolar Fluids over Vertical Non-Isothermal Surfaces, *Int. J. Engng Sci.*, 1990, **28**, pp. 783–792.
16. Gorla, R. S. R. and Takhar, H. S., Boundary Layer Flow of a Micropolar Fluid on Rotating Axisymmetric Surfaces with a Concentrated Heat Source, *Acta Mech.*, 1994, **105**, pp. 1–10.
17. Gorla, R. S. R. and Nashery, K., The Contributions of Microrotation of Lubricant Molecules in Modeling a Thin Film Journal Bearing, *Acta Mech.*, 2002, **158**, pp. 185–198.
18. Gorla, R. S. R., Slaouti, A., and Takhar, H. S., Free Convection in Micropolar Fluids over a Uniformly Heated Vertical Plate, *Int. J. Numer. Methods Heat Fluid Flow*, 1998, **8**, pp. 504–518.
19. Gorla, R. S. R., Takhar, H. S., and Slaouti, A., MHD Free Convection Boundary Layer Flow of a Micropolar Fluid over a Vertical Plate, *Int. J. Engng Sci.*, 1998, **36**, pp. 315–327.
20. Gorla, R. S. R., Poulos, E. N., and Byrd, L. W., Effect of Electrostatic Field on Rupture of Thin Micropolar Liquid Film, *Int. J. Fluid Mech. Resch*, 1999, **26**, pp. 425–436.
21. Hassanien, I. A., Moursy, N. M., and Gorla, R. S. R., Mixed Convection Flow of Micropolar Fluid on a Horizontal Plate Moving in Parallel to a Free Stream, *Int. J. Fluid Mech. Resch*, 2004, **31**, pp. 417–429.
22. Hassanien, I. A., and Gorla, R. S. R., Nonsimilar Solutions for Natural Convection in Microp-

olar Fluids on a Vertical Plate, *Int. J. Fluid Mech. Resch*, 2003, **30**, pp. 381–394.
23. Mohammadein, A. A., and Gorla, R. S. R., Heat Transfer in a Micropolar Fluid over a Stretching Sheet with Viscous Dissipation and Internal Heat Generation, *Int. J. Numer. Methods Heat Fluid Flow*, 2001, **11**, pp. 50–58.
24. Mohammadein, A. A., Modather, M., Salem, A., and Gorla, R. S. R., Mixed Convection Flow of a Micropolar Fluid on a Moving Heated Horizontal Plate, *ZAMM*, 2001, **81**, pp. 549–557.
25. Hossain, M. A., Chowdhury, M. K., and Gorla, R. S. R., Natural Convection of Thermomicropolar Fluid from an Isothermal Surface Inclined at a Small Angle to the Horizontal, *Int. J. Numer. Methods Heat Fluid Flow*, 1999, **9**, pp. 814–832.
26. Mansour, M. A., Mohammadein, A. A., El-Kabeir, S., and Gorla, R. S. R., Heat Transfer from Moving Surfaces in a Micropolar Fluid, *Can. J. Phys.*, 1999, **77**, pp. 1–9.
27. Hassanien, I. A., Shamardan, A., Moursy, N. M., and Gorla, R. S. R., Flow and Heat Transfer in the Boundary Layer of a Micropolar Fluid on a Continuous Moving Surface, *Int. J. Numer. Methods Heat Fluid Flow*, 1999, **9**, pp. 643–659.
28. Hossain, M. A., Chowdhury, M. K., and Gorla, R. S. R., Free Convection Flow of Thermomicropolar Fluid Along a Vertical Plate with Nonuniform Surface Temperature and Surface Heat Flux, *Int. J. Numer. Methods Heat Fluid Flow*, 1999, **9**, pp. 568–585.
29. Pop, I., Gorla, R. S. R., Rees, D. A. S., and Takhar, H. S., Convective Wall Plume in Micropolar Fluids, *ZAMM*, 1998, **78**, pp. 431–438.
30. Hassanien, I. A., Bakier, A. Y., and Gorla, R. S. R., Natural Convection Boundary Layer Flow of a Micropolar Fluid, *ZAMM*, 1997, **77**, pp. 751–755.
31. Mohammadien, A. A., and Gorla, R. S. R., Effects of Transverse Magnetic Field on Mixed Convection in Micropolar Fluid on a Horizontal Plate with Vectored Mass Transfer, *Acta Mech.*, 1996, **118**, pp. 1–12.
32. Arafa, A. A., and Gorla, R. S. R., Mixed Convection Boundary Layer Flow of a Micropolar Fluid Along Vertical Cylinders and Needles, *Int. J. Engng Sci.*, 1992, **30**, pp. 1745–1751.
33. Gebhart, B., Jaluria, Y., Mahajan, R. L., and Sammakia, B., *Buoyancy Induced Flows and Transport*, Hemisphere, New York, 1988.
34. Mansour, M. A. and Gorla, R. S. R., MHD Mixed Convection Boundary Layer Flow of a Micropolar Fluid from a Horizontal Cylinder, *Appl. Mech. Engng*, 1999, **4**, pp. 649–662.
35. Ahmadi, G., Self Similar Solution of Incompressible Micropolar Boundary Layer Flow over a Semi-infinite Flat Plate, *Int. J. Engng Sci.*, 1976, **14**, pp. 639–646.